One-Photon Mass-Analyzed Threshold Ionization Spectroscopy of *trans*- and *cis*-1-C_3H_5Br: Ionization Energies and Vibrational Assignments for the Cations

Mina Lee and Myung Soo Kim*

National Creative Research Initiative Center for Control of Reaction Dynamics and School of Chemistry, Seoul National University, Seoul 151-742, Korea

Received: September 22, 2003; In Final Form: October 20, 2003

Vibrational spectra of *trans*- and *cis*-1-C_3H_5Br cations in the ground electronic states were obtained by the one-photon mass-analyzed threshold ionization (MATI) spectroscopy using the coherent vacuum ultraviolet radiation generated by four-wave difference frequency mixing in Kr. From the MATI spectra, ionization energies of *trans*- and *cis*-1-C_3H_5Br to the ionic ground states have been determined to be 9.2693 ± 0.0006 and 9.3140 ± 0.0006 eV, respectively. Almost complete vibrational assignments for the peaks in the MATI spectra were possible by utilizing vibrational frequencies and Franck−Condon factors calculated at the B3LYP and BP86 levels with the 6-311++G(3df,3pd) basis set.

I. Introduction

Zero kinetic energy (ZEKE) photoelectron spectroscopy[1−5] is a useful technique to obtain vibrational and even rotational information on polyatomic cations. In ZEKE, a gaseous neutral is excited to a high Rydberg state lying very close to the ionization limit, usually via two-photon 1 + 1′ scheme[5] and ionized by pulsed electric field (pulsed field ionization, PFI). By scanning the frequency of the second (1′) laser and detecting the electron current, a ZEKE spectrum is recorded that is virtually the vibration−rotation spectrum of the corresponding cation. Mass-analyzed threshold ionization (MATI)[6−11] is its variation that detects the cation instead of the electron. The mass selectivity and the capability to generate state-selected molecular ions are the main advantages of the latter.[12,13]

Intermediate state selection in the two-photon scheme often provides useful information for vibrational assignments of ZEKE/MATI spectra. This scheme is not generally applicable, however, because the excited states of most polyatomic molecules cannot be accessed by one-photon absorption by use of a commercial dye laser and because those accessible often display diffuse spectra indicating rapid relaxation or dissociation.[14,15] We have been performing spectroscopy of the cations of some aliphatic halides as a preliminary step to generation of state-selected ions and study of their dissociation dynamics.[16,17] The two-photon scheme is not appropriate in these cases for the reasons described above. Such difficulties can be avoided in the one-photon scheme, which utilizes the vacuum ultraviolet radiation[18−20] generated by four-wave mixing, as demonstrated in our previous reports.[9−11]

Methyl rotor is an outstanding spectroscopic problem, which has relevance to chemical reaction dynamics.[21−26] The character of the torsional motion of a methyl group changes depending on its energy, from vibration at below the torsional barrier to free internal rotation at far above. In our previous MATI investigation of 2-bromopropene,[17] a rich vibrational structure was observed near the 0-0 band that could not be readily assigned through ordinary normal-mode analysis. Detailed theoretical study showed that the seemingly irregularly spaced peaks in the structure were due to transitions to the torsional/internal rotational states and that the torsional barrier of this molecule was lowered dramatically upon ionization.

The MATI spectroscopic investigation of *trans*- and *cis*-1-bromopropenes is presented in this paper. Accurate ionization energies to the ground-state cations and vibrational assignments will be reported. Results from the theoretical calculations of the torsional energy levels of the neutrals and the cations of the two isomers will be reported also. These have relevance to spectral interpretation even though the irregularly spaced torsional overtones have not been observed in the present cases.

II. Experimental Section

trans- and *cis*-1-C_3H_5Br with 99% and 97% purity, respectively, were purchased from Sigma Aldrich and used without further purification. Gaseous samples at ambient temperature were seeded in Ar at the stagnation pressure of ∼2 atm and supersonically expanded through a pulsed nozzle (diameter 500 μm, General Valve). The supersonic beam was then introduced to the ionization chamber through a skimmer (diameter 1 mm, Beam Dynamics) placed about 3 cm downstream from the nozzle orifice. The typical background pressure in the ionization chamber was $\sim 7 \times 10^{-8}$ Torr.

The method to generate a vacuum UV pulse by four-wave difference frequency mixing in Kr was explained in detail previously[9−11] and will not be repeated here. The vacuum UV laser pulse was collinearly overlapped with the molecular beam in a counterpropagation manner and slit electrodes were used to collect the ions efficiently. Weak spoil field was applied to remove the directly produced ions. To achieve the pulsed-field ionization (PFI) of the neutrals in ZEKE states,[9,10] the electric field of 15−90 V/cm was applied at a certain delay time after the vacuum UV pulse. The ions generated were then accelerated, flown through a field-free region, and were detected. Scrambling field was applied to lengthen the lifetime of ZEKE states.

To cover the full vibrational spectral range (0∼3500 cm^{-1}) of the 1-$C_3H_5Br^+$ cation, it was necessary to use the outputs from several dye lasers in the generation of vacuum UV. The dye laser output affected the vacuum UV power, which, in turn,

* To whom correspondence should be addressed: e-mail myungsoo@plaza.snu.ac.kr; tel +82-2-880-6652; fax +82-2-889-1568.

10.1021/jp0368278 CCC: $25.00
Published on Web 11/26/2003

affected the signal intensity in a MATI spectrum. Since comparing the relative intensities of each vibrational peak obtained by experiment and by theoretical calculation was one of the main tools for spectral assignment in this work, it was necessary to calibrate the peak intensity with the vacuum UV power. For this purpose, a thin gold wire was placed in the vacuum UV beam path to intercept a small portion of it. The photoelectric current from the monitor, measured while vacuum UV was scanned, was used for calibration.[27] It is to be mentioned, however, that the vacuum UV power did not change much in the spectral range covered (10% or less) as far as the effective spectral region for each dye was used.

III. Computational Section

Quantum chemical calculations were done for *trans*- and *cis*-1-C_3H_5Br neutrals and cations in the ground electronic states at the B3LYP and BP86 density functional theory (DFT) levels using the Gaussian 98 suite of programs.[28] Even though the calculations were done at the Hartree−Fock and Møller−Plesset perturbation theory levels also, the results were not as compatible with the experimental data as the DFT results. The size of the basis set was systematically increased until the basis-set dependence disappeared. Equilibrium geometries, Hessians, and vibrational frequencies were calculated. Also calculated were the barriers for the methyl torsional motion. Here electronic energy was calculated at the optimized geometry for a specified torsional angle, which was varied systematically.

The method to calculate the Franck−Condon factors in a MATI process from the quantum chemical results was described in detail previously.[16,17] Only a brief account of the procedure will be presented here. Assuming that the ion core in a high Rydberg state is essentially the same as the corresponding cation, the vibrational wave function of the latter was used in the calculation of the vibrational overlap integral. Product of the harmonic oscillator eigenfunctions for each normal mode was used as the vibrational wave function. Since the normal coordinates changed upon ionization, it was needed to relate those in the initial (**Q**′′) and final (**Q**′) states, which was accomplished as follows.[29,30]

$$\mathbf{Q}'' = \mathbf{J}\mathbf{Q}' + \mathbf{K} \tag{1}$$

J is called the Duschinsky matrix, which represents changes in the normal mode pattern, while **K** represents changes in the equilibrium geometry upon ionization. **Q**′′ and **Q**′ obtained by the DFT calculations were expressed with common internal coordinates to evaluate **J** and **K**.[29] Atomic numberings for the *trans*- and *cis*-1-C_3H_5Br are shown in Figure 1. The internal coordinates chosen were eight bond lengths, seven bond angles formed by H(1)C(1)C(2), BrC(1)C(2), C(1)C(2)C(3), C(1)C(2)H(2), C(2)C(3)H(3), C(2)C(3)H(4), and C(2)C(3)H(5), and six dihedral angles formed by H(1)C(1)C(2)C(3), BrC(1)C(2)C(3), BrC(1)C(2)H(2), H(2)C(2)C(3)H(3), H(2)C(2)C(3)H(4), and H(2)C(2)C(3)H(5). Then, the overlap integrals and hence the Franck−Condon factors were calculated from the analytical expressions in ref 29.

The method to calculate the torsional/internal rotational energy levels is available in the literature.[31,32] The torsional Hamiltonian operator is given by

$$\hat{H} = -B\frac{\partial^2}{\partial\phi^2} + V(\phi) \tag{2}$$

Here ϕ is the torsional angle, B is the reduced internal rotational constant, and $V(\phi)$ is the one-dimensional torsional potential.

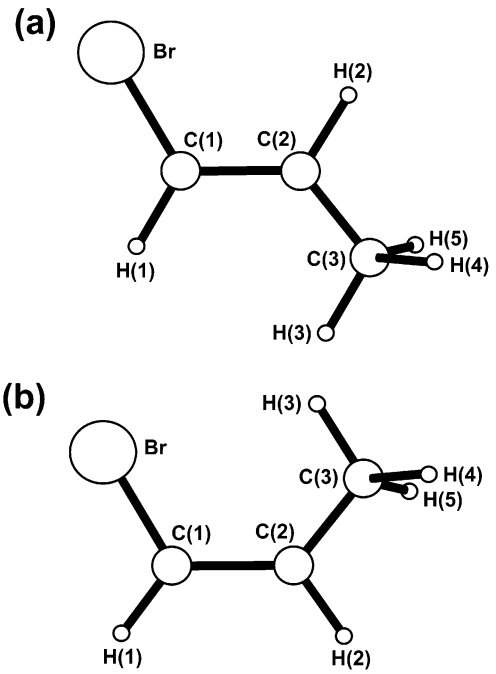

Figure 1. Atomic numberings for (a) *trans*-1-C_3H_5Br and (b) *cis*-1-C_3H_5Br.

The following periodic form of $V(\phi)$ was used:

$$V(\phi) = \frac{V_3}{2}(1 - \cos 3\phi) \tag{3}$$

The torsional barrier obtained by DFT calculation was taken as V_3. The Hamiltonian matrix was constructed from one-dimensional free rotor eigenfunctions, cos ($m\phi$) and sin ($m\phi$), and diagonalized to obtain torsional/internal rotational energy levels.

IV. Results and Discussion

A. Quantum Chemical Calculations. At all the levels used in the calculation, the equilibrium geometries of the neutrals and the cations of *trans*- and *cis*-1-C_3H_5Br had planar symmetry, C_s. Considering the valence orbitals only, the electron configurations of the ground-state neutrals of both isomers are ...$(1a'')^2$-$(9a')^2(2a'')^2$, resulting in $\tilde{X}^1A'$. Here $2a''$ is a π orbital with C═C bonding and C−Br antibonding character. $9a'$ and $1a''$ are the bromine 4p nonbonding orbitals parallel and perpendicular to the molecular plane, respectively, n($Br4p_{||}$) and n($Br4p_{\perp}$). The ground-state cations of both isomers, $\tilde{X}^2A''$, are formed by removal of an electron from $2a''$.

The equilibrium geometries of the neutrals and the cations of *trans*- and *cis*-1-C_3H_5Br in the ground states obtained at the B3LYP and BP86 levels with the 6-311++G(3df,3pd) basis set are listed in Tables 1 and 2, respectively. Structural data determined for the trans isomer by microwave spectroscopy[33] are also listed in Table 1, which are in good agreement with the calculated results. In our earlier MATI investigations, geometrical changes upon ionization were utilized for the qualitative explanation of the vibrational band intensities in a MATI spectrum.[16,17] These are listed in the above tables also. The most prominent changes upon ionization for both isomers are lengthening of the C(1)═C(2) bond length and shortening of the C(1)−Br bond length. Changes in these bond lengths are compatible with the character of the orbital from which an electron is removed, $2a''$. The C(2)−C(3) bond length decreases

TABLE 1: Geometries of *trans*-1-C_3H_5Br Neutral and Cation in the Ground Electronic State[a]

	neutral ($\tilde{X}^1A'$)			cation ($\tilde{X}^2A''$)	
C_s	exp[b]	B3LYP	BP86	B3LYP	BP86
		Interatomic Distance (Å)			
C(1)−C(2)	1.336	1.322	1.333	1.387 (0.065)	1.393 (0.060)
C(2)−C(3)	1.501	1.498	1.501	1.459 (-0.039)	1.460 (−0.041)
C(1)−Br	1.884	1.905	1.907	1.820 (−0.086)	1.830 (−0.077)
C(1)−H(1)	1.091	1.080	1.089	1.083 (0.003)	1.092 (0.003)
C(2)−H(2)	1.090	1.084	1.093	1.086 (0.002)	1.095 (0.002)
C(3)−H(3)	1.090	1.089	1.098	1.086 (−0.003)	1.094 (−0.004)
C(3)−H(4)	1.090	1.092	1.101	1.100 (0.008)	1.110 (0.009)
		Bond Angle (deg)			
C(1)−C(2)−C(3)	124.3	123.5	123.3	123.5 (0.0)	123.2 (0.0)
C(1)−C(2)−H(2)	119.0	119.4	119.3	118.1 (−1.3)	118.2 (−1.2)
C(2)−C(1)−Br	122.1	123.5	123.5	121.8 (−1.7)	121.7 (−1.8)
C(2)−C(1)−H(1)	120.5	124.3	124.3	122.6 (−1.7)	123.0 (−1.3)
Br−C(1)−H(1)	117.4	112.2	112.2	115.6 (3.4)	115.4 (3.1)
C(2)−C(3)−H(3)		111.9	111.9	114.5 (2.6)	114.9 (3.0)
C(2)−C(3)−H(4)		110.7	110.8	109.0 (−1.7)	109.1 (−1.7)
H(4)−C(3)−H(5)	107.7	106.9	106.8	103.3 (−3.6)	102.1 (−4.6)
		Dihedral Angle (deg)			
C(1)−C(2)−C(3)−H(4)		120.8	120.8	124.0 (3.2)	124.6 (3.7)

[a] Calculated at the B3LYP and BP86 levels with the 6-311++G(3df,3pd) basis set. Geometrical changes upon ionization are shown in parentheses. [b] Microwave spectroscopic results in ref 33.

TABLE 2: Geometries of *cis*-1-C_3H_5Br Neutral and Cation in the Ground Electronic State[a]

	neutral ($\tilde{X}^1A'$)		cation ($\tilde{X}^2A''$)	
C_s	B3LYP	BP86	B3LYP	BP86
	Interatomic Distance (Å)			
C(1)−C(2)	1.324	1.334	1.392 (0.068)	1.398 (0.063)
C(2)−C(3)	1.492	1.494	1.455 (−0.037)	1.456 (−0.039)
C(1)−Br	1.908	1.911	1.819 (−0.089)	1.830 (−0.081)
C(1)−H(1)	1.078	1.088	1.082 (0.004)	1.091 (0.004)
C(2)−H(2)	1.086	1.096	1.087 (0.001)	1.097 (0.001)
C(3)−H(3)	1.087	1.097	1.084 (−0.002)	1.094 (−0.003)
C(3)−H(4)	1.092	1.101	1.100 (0.007)	1.110 (0.009)
	Bond Angle (deg)			
C(1)−C(2)−C(3)	128.5	128.2	128.3 (−0.2)	128.2 (0.0)
C(1)−C(2)−H(2)	114.9	114.8	114.3 (−0.6)	114.2 (−0.7)
C(2)−C(1)−Br	124.9	124.5	124.0 (−0.9)	123.7 (−0.8)
C(2)−C(1)−H(1)	123.5	123.8	121.2 (−2.3)	121.8 (−2.1)
Br−C(1)−H(1)	111.6	111.7	114.8 (3.2)	114.6 (2.9)
C(2)−C(3)−H(3)	111.9	111.7	115.0 (3.0)	115.2 (3.5)
C(2)−C(3)−H(4)	110.5	110.7	108.7 (−1.8)	108.9 (−1.7)
H(4)−C(3)−H(5)	106.8	106.6	103.2 (−3.6)	102.1 (−4.5)
	Dihedral Angle (deg)			
C(1)−C(2)−C(3)−H(4)	121.0	121.0	124.2 (3.1)	124.7 (3.7)

[a] Calculated at the B3LYP and BP86 levels with the 6-311++G(3df,3pd) basis set. Geometrical changes upon ionization are shown in parentheses.

upon ionization, indicating that $2a''$ also has some antibonding character to this bond. Changes in the bond angles upon ionization are similar for the two isomers, even though no simple explanation based on the orbital picture can be made for the trend. For 2-C_3H_5Br reported previously,[17] the increase in the C(3)C(2)Br bond angle was the main change upon ionization [the atomic numbering for this isomer is obtained by exchanging H(2) and Br in Figure 1].

The harmonic vibrational frequencies of the trans and the cis neutrals calculated at the B3LYP and BP86 levels are listed in Tables 3 and 4, respectively, together with the experimental data.[34] Reassignment has been made for some experimental data, which will be explained later. Also listed in the tables are the frequencies of the torsional fundamentals calculated by the quantum mechanical method described in the previous section. Similar data for the cations are listed in Tables 5 and 6. The main characters of each normal modes of the neutrals are listed in Tables 3 and 4 also. When the modes are numbered according to the Mulliken convention, the same type vibrations of the neutrals and cations are designated by different mode numbers in some cases. Also, the mode number for the CH_3 torsion changes depending on the frequency used, harmonic or quantum mechanical. To avoid confusion, the mode numbering for the cis neutral will be adopted throughout, the vibrations with the same character for the other systems being designated by the same mode number.

The vibrational frequencies of the neutrals measured from their infrared and Raman spectra reported by Elst et al.,[34] after some reassignments, are in excellent agreement with the calculated results. For most of the low- to medium-frequency modes, experimental data lie between the B3LYP and BP86 results. The same trend, which probably arises from different error cancellations at the two DFT levels,[35] was also observed in our previous study of 2-C_3H_5Br and utilized advantageously in the mode assignment.[17]

Accepting the reliability of the DFT frequencies, one finds that the assignment of weak peaks at 677 cm^{-1} in the spectra of the trans isomer to ν_{20} (out-of-plane bending) made by Elst

TABLE 3: Vibrational Frequencies of *trans*-1-C_3H_5Br Neutral in the Ground Electronic State[a]

		neutral ($\tilde{X}^1A'$)			
mode[b]	symm	exp[c]	B3LYP	BP86	mode character
1	a'	3078	3206	3127	CH stretching
2	a'	3029	3160	3086	CH stretching
3	a'	2980	3102	3036	CH stretching
4	a'	2937	3019	2948	CH stretching
5	a'	1637	1685	1627	C═C stretching
6	a'	1461	1486	1433	CH_3 deformation
7	a'	1387	1415	1359	CH_3 deformation
8	a'	1292	1323	1274	in-plane C−C stretching/ CCH bending
9	a'	1225	1251	1202	in-plane C−C stretching/ CCH bending
10	a'	1087	1101	1069	in-plane C−C stretching/ CCH bending
11	a'	952	954	928	CH_3 deformation
12	a'	729	720	702	CBr stretching
13	a'	355	351	342	CCBr/CCC bending
14	a'	250	236	227	CCBr/CCC bending
15	a''	2961	3065	2997	CH stretching
16	a''	1446	1480	1427	out-of-plane bending
17	a''	1041	1070	1023	out-of-plane bending
18	a''	931	966	925	out-of-plane bending
19	a''	743	772	734	out-of-plane bending
20	a''	210	197	192	out-of-plane bending
21	a''		221 (170)[d]	216 (167)[d]	CH_3 torsion

[a] Calculated at the B3LYP and BP86 levels with the 6-311++G(3df,3pd) basis set. Vibrational frequencies are given in reciprocal centimeters. [b] Mode numberings for the cis neutral were adopted. [c] Infrared absorption spectroscopic data in ref 34 after reassignment. See text for the details of the reassignment made. [d] Frequency calculated by the quantum mechanical method is shown in parentheses.

TABLE 4: Vibrational Frequencies of *cis*-1-C_3H_5Br Neutral in the Ground Electronic State[a]

		neutral ($\tilde{X}^1A'$)			
mode[b]	symm	exp[c]	B3LYP	BP86	mode character
1	a'	3102	3224	3145	CH stretching
2	a'	3034	3136	3060	CH stretching
3	a'	2978	3121	3044	CH stretching
4	a'	2947	3025	2951	CH stretching
5	a'	1638	1687	1632	C═C stretching
6	a'	1456	1481	1428	CH_3 deformation
7	a'	1388	1415	1359	CH_3 deformation
8	a'	1312	1336	1285	in-plane C−C stretching/ CCH bending
9	a'	1212	1247	1202	in-plane C−C stretching/ CCH bending
10	a'	1070	1083	1044	in-plane C−C stretching/ CCH bending
11	a'	936	933	913	CH_3 deformation
12	a'	677	676	660	CBr stretching
13	a'	494	490	478	CCBr/CCC bending
14	a'	194	194	187	CCBr/CCC bending
15	a''	2960	3067	2998	CH stretching
16	a''	1444	1485	1432	out-of-plane bending
17	a''	1041	1066	1022	out-of-plane bending
18	a''	925	954	904	out-of-plane bending
19	a''	684	692	665	out-of-plane bending
20	a''	382	394	381	out-of-plane bending
21	a''		102 (97)[d]	113 (100)[d]	CH_3 torsion

[a] Calculated at the B3LYP and BP86 levels with the 6-311++G(3df,3pd) basis set. Vibrational frequencies are given in reciprocal centimeters. [b] Mulliken notation. [c] Infrared absorption spectroscopic data in ref 34 after reassignment. See text for the details of the reassignment made. [d] Frequency calculated by the quantum mechanical method is shown in parentheses.

et al.[34] is troublesome because its DFT prediction is ~195 cm^{-1}. Our own infrared spectroscopic measurement showed a very weak peak at ~677 cm^{-1} also. Its intensity grew, even though slowly, after the sample was exposed to the atmosphere. Moreover, peaks at ~677 cm^{-1} were the most intense peaks in the infrared and Raman spectra of the cis isomer reported by Elst et al. Namely, it is highly likely that the weak peaks at 677 cm^{-1} in the trans spectra were due to cis contamination. With the 677 cm^{-1} peak eliminated, the very weak peaks observed at 210 and 194 cm^{-1} in the infrared and Raman spectra, respectively, of the trans isomer reported by Elst et al. can be assigned either to CH_3 torsion or to an out-of-plane bending. We will adopt the latter assignment and assume that the torsional fundamental expected at ~170 cm^{-1} from the quantum mechanical calculations was not detected in the above vibrational spectra because the measurements were done above 200 cm^{-1}.

The vibrational assignments for the cis isomer reported by Elst et al.[34] are in serious disagreement with the DFT results. The peaks at 765, 684, 677, 494, and 194 cm^{-1} were assigned to the fundamentals of modes 12, 13, 19, 14, and 21, respectively, while DFT calculations predict these to appear at around 670, 480, 680, 190, and 110 cm^{-1}. The good agreement between the experimental and calculated frequencies can be achieved, however, when the experimental peaks at 684, 677, 494, and 194 cm^{-1} are assigned to the fundamentals of modes 19, 12, 13, and 14, which have DFT frequencies of around 680, 670, 480, and 190 cm^{-1}, respectively. Then, the very weak peak at ~765 cm^{-1} observed by Elst et al. must be due to the first overtone of mode 20 (382 cm^{-1} × 2). After reassignments, experimental and calculated frequencies are in excellent agreement as can be seen in Tables 3 and 4.

In the case of 2-C_3H_5Br reported previously, the torsional barrier was found to be lowered dramatically upon ionization, from 907 cm^{-1} in the neutral to 80 cm^{-1} in the cation.[17] This caused the appearance of irregular torsion/internal rotation overtones in the MATI spectrum. The possibility of similar complication in the MATI spectra of 1-C_3H_5Br isomers has been checked by use of the torsional barriers (V_3) and the reduced internal rotation constants (B) obtained by quantum chemical calculations. V_3 and B for the neutrals and the cations of 1-C_3H_5-Br isomers obtained at the B3LYP level are listed in Table 7. Even though the torsional barriers change substantially upon ionization for both the trans and the cis isomers, the changes are not as dramatic as for 2-C_3H_5Br (from 907 to 80 cm^{-1}). Hence, splitting of torsional levels is not significant for the neutrals and the cations of 1-C_3H_5Br isomers as can be seen from the energy level data listed in Table 7 calculated with the parameters in the same table. It is to be noted, however, that taking the torsional barriers into account results in torsional energy levels that are significantly different from those expected under the harmonic approximation.

B. One-Photon MATI Spectra and Ionization Energies. The one-photon MATI spectra of *trans*- and *cis*-1-C_3H_5Br recorded by monitoring $C_3H_5{}^{79}Br^+$ generated in the ground electronic state are shown in Figures 2 and 3, respectively. The spectra recorded by monitoring $C_3H_5{}^{81}Br^+$ were hardly different because the calculated isotopic shifts were much smaller than the bandwidth and hence are not shown. The spectra magnified along the y direction are shown as insets to demonstrate the quality of the spectra.

The most intense peaks, appearing at ~74 758 and ~75 119 cm^{-1} in Figures 2 and 3, respectively, correspond to the 0-0 bands. The position of the 0-0 band in one-photon MATI

TABLE 5: Vibrational Frequencies[a] and Their Assignments for *trans*-1-C_3H_5Br Cation in the Ground Electronic State ($\tilde{X}^2A''$)

		B3LYP[b]		BP86[b]		MATI	
mode[c]	symm	freq	int[d]	freq	int[d]	freq	int[e]
			Fundamentals				
1	a'	3198	1×10^{-5}	3120	1×10^{-5}		
2	a'	3169	3×10^{-7}	3094	9×10^{-5}		
3	a'	3146	5×10^{-4}	3078	4×10^{-4}		
4	a'	2970	0.002	2892	0.003	2970[f]	0.006
5	a'	1533	0.285	1484	0.259	1493	0.112
6	a'	1446	0.234	1395	0.214	1402[f]	0.083
7	a'	1334	1×10^{-4}	1273	0.010	1308	0.009
8	a'	1292	0.333	1249	0.260	1267	0.130
9	a'	1276	0.002	1224	0.011	1194	0.009
10	a'	1157	0.001	1131	0.002	1124	0.014
11	a'	942	0.001	918	0.001	942	0.011
12	a'	791	0.319	765	0.285	787	0.163
13	a'	371	0.376	361	0.329	370	0.364
14	a'	242	0.200	232	0.206	238	0.228
15	a''	2990	0	2907	0		
16	a''	1416	0	1349	0	1357	0.008
17	a''	1012	0	962	0		
18	a''	849	0	817	0	876	0.013
19	a''	780	0	745	0	752	0.029
20	a''	146	0	143	0	141	0.043
21	a''	164	1×10^{-8}	164	1×10^{-8}	154	0.028
		(144)[g]		(144)[g]			
			Overtones and Combinations				
20^2		291	0.016	285	0.016	276	0.038
21^2		327	0.013	329	0.010	303	0.052
		(272)[g]		(273)[g]			
14^2		484	0.019	465	0.020	477	0.017
13^120^1		517	0	504	0	511	0.017
13^114^1		613	0.083	593	0.075	608	0.048
13^120^2		662	0.006	646	0.005	643	0.009
13^121^2		698	0.005	690	0.003	674	0.010
		(643)[g]		(634)[g]			
13^2		742	0.083	722	0.064	740	0.038
13^114^2		855	0.009	826	0.008	823	0.016
13^214^1		984	0.020	954	0.016	981	0.013
12^114^1		1033	0.064	998	0.058	1026	0.033
12^120^2		1082	0.005	1050	0.005	1063	0.015
12^121^2		1118	0.004	1094	0.003	1093	0.014
		(1063)[g]		(1038)[g]			
12^113^1		1162	0.130	1126	0.101	1157	0.058
$12^113^114^1$		1404	0.028	1359	0.023	1402[e]	0.083
12^2		1582	0.068	1531	0.054	1578	0.029
6^114^1		1688	0.046	1627	0.043	1616	0.020
8^113^1		1663	0.137	1610	0.093	1640	0.048
5^114^1		1774	0.059	1717	0.055	1735	0.019
6^113^1		1817	0.094	1756	0.075	1773	0.025
5^113^1		1904	0.115	1845	0.092	1865	0.027
12^213^1		1953	0.029	1892	0.020	1950	0.006
8^112^1		2083	0.111	2015	0.079	2060	0.015
$5^113^114^1$		2146	0.026	2078	0.021	2103	0.007
6^113^2		2188	0.022	2117	0.015	2147	0.006
6^112^1		2237	0.079	2160	0.063	2193	0.020
5^113^2		2275	0.027	2206	0.019	2233	0.009
5^112^1		2324	0.098	2250	0.078	2284	0.025
$8^112^113^1$		2454	0.049	2376	0.030	2430	0.007
$5^112^114^1$		2565	0.018	2482	0.017	2521	0.008
8^2		2585	0.048	2499	0.029	2535	0.007
$6^112^113^1$		2608	0.023	2521	0.024	2561	0.004
6^18^1		2738	0.066	2644	0.047	2671	0.009
5^18^1		2825	0.076	2734	0.056	2757	0.015
6^2		2892	0.026	2789	0.022	2801	0.006
5^16^1		2979	0.055	2879	0.044	2892	0.012
5^2		3065	0.034	2969	0.028	2970[e]	0.006
5^112^2		3114	0.022	3015	0.016	3051	0.005
6^213^1		3263	0.011	3150	0.008	3138	0.005
$5^16^113^1$		3350	0.024	3240	0.017	3273	0.004

[a] Vibrational frequencies are given in reciprocal centimeters. [b] With the 6-311++G(3df,3pd) basis set. [c] Mode numberings for the cis neutral were adopted. [d] Franck−Condon factor for each transition normalized to that of the 0-0 transition. [e] Peak intensity normalized to that of the 0-0 band. [f] Overlapping bands. [g] Numbers in parentheses are the theoretical frequencies from quantum mechanical results for mode 21 in Table 7.

TABLE 6: Vibrational Frequencies[a] and Their Assignments for *cis*-1-C_3H_5Br Cation in the Ground Electronic State ($\tilde{X}^2A''$)

		B3LYP[b]		BP86[b]		MATI	
mode[c]	symm	freq	int[d]	freq	int[d]	freq	int[e]
			Fundamentals				
1	a'	3206	3×10^{-5}	3128	3×10^{-5}		
2	a'	3166	3×10^{-4}	3092	4×10^{-4}		
3	a'	3146	6×10^{-6}	3065	3×10^{-6}		
4	a'	2976	0.002	2896	0.003		
5	a'	1539	0.270	1494	0.266	1506	0.095
6	a'	1436	0.234	1384	0.209	1397	0.104
7	a'	1325	0.155	1266	0.158	1263[f]	0.107
8	a'	1366	0.089	1312	0.073	1302	0.070
9	a'	1266	0.120	1225	0.048	1235	0.107
10	a'	1110	0.101	1072	0.101	1087[f]	0.044
11	a'	916	0.000	898	0.009		
12	a'	737	0.186	717	0.151	743	0.263
13	a'	521	0.377	506	0.340	519	0.338
14	a'	201	0.017	193	0.006	204	0.028
15	a''	2996	0	2912	0		
16	a''	1415	0	1347	0	1341	0.026
17	a''	1011	0	963	0	984[f]	0.023
18	a''	839	0	800	0	804	0.014
19	a''	730	0	704	0	706	0.028
20	a''	241	0	234	0	235	0.037
21	a''	129	1×10^{-6}	142	1×10^{-6}		
		(141)[g]		(148)[g]			
			Overtones and Combinations				
21^2		257	0.004	283	0.003	223	0.045
		(267)[g]		(280)[g]			
20^121^1		370	0.002	376	0.004	347	0.006
		(382)[g]		(382)[g]			
20^2		483	0.030	469	0.029	475	0.059
20^221^1		611	0	610	0	589	0.006
		(624)[g]		(617)[g]			
13^121^1		650	0	647	0	626	0.010
		(662)[g]		(654)[g]			
12^114^1		938	0.004	910	0.001	942[f]	0.028
19^120^1		972	0.000	938	0.000	942[f]	0.028
13^120^2		1004	0.011	974	0.010	984[f]	0.023
13^2		1042	0.083	1012	0.068	1039	0.061
17^121^1		1139	0.003	1104	0.003	1105[f]	0.041
		(1152)[g]		(1111)[g]			
12^120^2		1004	0.011	1186	0.004	1216	0.062
12^113^1		1258	0.084	1223	0.063	1263[f]	0.107
$12^113^114^1$		1459	0.002	1416	0.001	1454	0.046
12^2		1475	0.028	1434	0.020	1484	0.103
13^3		1563	0.014	1517	0.010	1556	0.014
10^113^1		1632	0.040	1578	0.036	1618	0.018
9^120^2		1748	0.004	1694	0.001	1698	0.016
7^120^2		1808	0.005	1735	0.005	1739[f]	0.027
13^219^1		1773	0	1715	0	1739[f]	0.027
9^113^1		1787	0.048	1731	0.017	1751	0.030
7^113^1		1846	0.064	1772	0.059	1776	0.034
8^113^1		1887	0.036	1818	0.027	1819	0.037
13^116^1		1936	0	1853	0	1860	0.032
6^113^1		1957	0.093	1890	0.075	1913	0.037
9^112^1		2003	0.025	1942	0.008	1985[f]	0.032
7^112^1		2062	0.033	1983	0.026	1985[f]	0.032
5^113^1		2060	0.109	1999	0.096	2030	0.040
12^116^1		2152	0	2064	0	2081	0.025
6^112^1		2173	0.046	2101	0.033	2137	0.029
12^3		2212	0.004	2151	0.002	2219	0.014
5^112^1		2277	0.056	2211	0.045	2255	0.022
9^110^1		2376	0.011	2297	0.004	2328	0.011
6^116^1		2850	0	2731	0	2732	0.010
5^16^1		2975	0.051	2878	0.044	2899	0.008

[a] Vibrational frequencies are given in reciprocal centimeters. [b] With the 6-311++G(3df,3pd) basis set. [c] Mode numberings for the cis neutral were adopted. [d] Franck−Condon factor for each transition normalized to that of the 0-0 transition. [e] Peak intensity normalized to that of the 0-0 band. [f] Overlapping bands. [g] Numbers in parentheses are the theoretical frequencies from quantum mechanical results for mode 21 in Table 7.

TABLE 7: Torsional Barriers (V_3), Reduced Internal Rotational Constants (B), and Torsional Energy Levels up to $v = 3$ for the Neutrals and Cations of *trans*- and *cis*-1-C_3H_5Br in the Ground Electronic State[a]

	trans-1-C_3H_5Br		*cis*-1-C_3H_5Br	
	neutral	cation	neutral	cation
V_3	694.4	513.0	256.1	498.1
B	5.38	5.33	5.38	5.33
$v = 0$	0.0000	0.0000	0.0000	0.0000
	0.0004(2)	0.0025(2)	0.0733(2)	0.0031(2)
$v = 1$	170.27(2)	143.66(2)	96.67(2)	141.34(2)
	170.29	143.77	98.56	141.47
$v = 2$	325.4	270.8	167.5	265.9
	325.9(2)	272.6(2)	180.2(2)	267.9(2)
$v = 3$	461.2(2)	374.9(2)	230.1(2)	367.1(2)
	466.3	390.0	277.9	383.6

[a] Evaluated at the B3LYP level with the 6-311++G(3df,3pd) basis set, in reciprocal centimeters. Numbers in parentheses denote degeneracy.

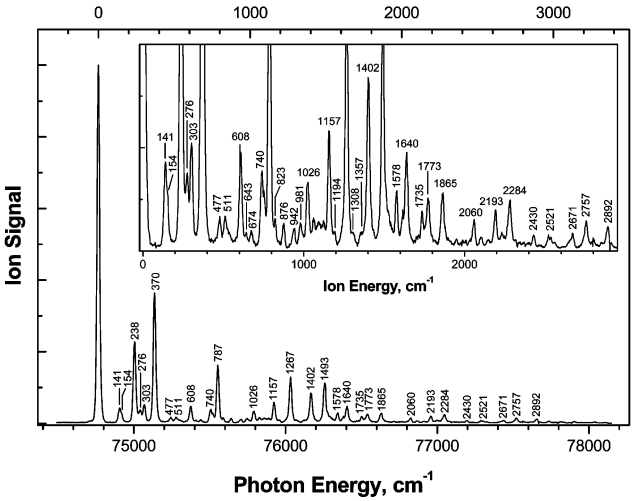

Figure 2. One-photon MATI spectrum of *trans*-1-C_3H_5Br recorded by monitoring $C_3H_5{}^{79}Br^+$ in the ground electronic state. The *x*-scale at the top of the figure corresponds to the vibrational frequency scale for the cation. Its origin is at the 0-0 band position. The spectrum in the 0∼3000 cm^{-1} region magnified by 10 is shown as an inset.

spectrum is equivalent to ionization energy. In practice, it is lower than the correct ionization energy, however, because the neutrals in the ZEKE states lying some cm^{-1} below the threshold can also be ionized when high PFI field is used. To correct for this effect, the 0-0 position was measured at various PFI fields and the results were extrapolated to the zero field limit. Spoil field was not used in such measurements. The ionization energies thus determined were 9.2693 ± 0.0006 and 9.3140 ± 0.0006 eV, respectively, for *trans*- and *cis*-1-C_3H_5Br. There are no data on the accurate ionization energies to the ground electronic states measured by ZEKE or MATI for these molecules. The only available one is 9.30 ± 0.05 eV[36] determined by photoionization for a mixture of the two isomers. The ionization energy data are listed in Table 8.

C. Vibrational Spectra for the Cations. Assuming that the shift of a vibrational peak in a MATI spectrum due to the applied electric field is similar to that of the 0-0 band, the vibrational frequency corresponding to each peak can be estimated simply by taking the difference of its position from that of the 0-0 band. The frequencies measured from the MATI spectra of the trans and cis isomers are listed in Tables 5 and 6, respectively. The vibrational frequency scales with the origins at the 0-0 band positions are also drawn in Figures 2 and 3. The vibrational

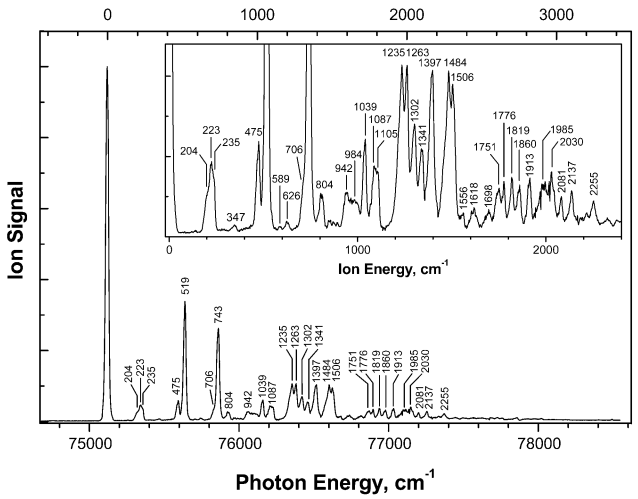

Figure 3. One-photon MATI spectrum of *cis*-1-C_3H_5Br recorded by monitoring $C_3H_5{}^{79}Br^+$ in the ground electronic state. The *x*-scale at the top of the figure corresponds to the vibrational frequency scale for the cation. Its origin is at the 0-0 band position. The spectrum in the 0∼2400 cm^{-1} region magnified by 7 is shown as an inset.

TABLE 8: Ionization Energies to the Ground Electronic States of *trans*- and *cis*-1-C_3H_5Br Cation

	IE (eV)	source
trans-1-C_3H_5Br	9.2693 ± 0.0006	this work
cis-1-C_3H_5Br	9.3140 ± 0.0006	this work
1-C_3H_5Br[a]	9.30 ± 0.05	PI[b]

[a] Data for *trans*- and *cis*-1-C_3H_5Br mixture in ref 36. [b] Photoionization.

peak intensities in the one-photon MATI spectra normalized to those of the 0-0 bands are also listed in the tables together with the calculated Franck−Condon factors normalized similarly.

In ZEKE/MATI, one can always choose a Rydberg state with proper symmetry such that the Rydberg ← ground transition is electric dipole-allowed.[37,38] Because most of the neutral molecules are at the zero point level, which is totally symmetric, a', under supersonic expansion condition, all the fundamental and overtone transitions of the totally symmetric modes, a', are dipole-allowed under the Born−Oppenheimer approximation. For the non-totally symmetric modes, a'', only the even-numbered overtones ($v = 2, 4, 6, ...$) are dipole-allowed. The calculated Franck−Condon factors for the fundamentals of these modes are zero, even though they may appear weakly in a ZEKE/MATI spectrum through vibronic mechanism.[14]

Before detailed analysis, it must be assured that a peak in a MATI spectrum is authentic and is not due to other contaminants. The mass-selective detection in MATI means that one usually has to worry about the contamination by isomers only, such as 2-C_3H_5Br, 3-C_3H_5Br, and *cyclic*-C_3H_5Br and the cross-contamination of the trans and the cis isomers in the present cases. The possibility of contamination by 3-C_3H_5Br and *cyclic*-C_3H_5Br can be readily eliminated because their ionization energies,[39,40] 10.01 and 9.93 eV, respectively, are much larger than those of the two 1-C_3H_5Br isomers. The ionization energy of 2-C_3H_5Br measured in this laboratory[16] is 9.4377 eV (∼76 115 cm^{-1}), which corresponds to the position of the strong 0-0 band. If samples were contaminated by 2-C_3H_5Br, the 0-0 band due to 2-C_3H_5Br would appear at 1358 and 997 cm^{-1} in the MATI spectra of *trans*- and *cis*-1-C_3H_5Br, respectively. Lack of the latter in Figure 3 ensures that the cis sample is quite free from contamination by 2-C_3H_5Br. There is a tiny peak at 1357 cm^{-1} in Figure 2, suggesting possible contamination of the trans

sample by 2-C_3H_5Br. However, the absence of other strong MATI peaks of 2-C_3H_5Br such as 13^1 expected at 1706 cm^{-1} in Figure 2 eliminates such a possibility. The cross-contamination of trans and cis isomers can be checked similarly. In this case, the 0-0 band of the cis isomer would appear at 361 cm^{-1} in the MATI spectrum of trans, and trans at -361 cm^{-1} in the cis spectrum. These peaks are hardly noticeable in the MATI spectra recorded.

1. *trans*-1-C_3H_5Br. Among 21 normal modes of 1-C_3H_5Br, 14 belong to a'. The transitions to the $v = 1$ levels of these modes, namely, fundamentals, are electric dipole-allowed and may appear distinctly in the one-photon MATI spectrum. From the calculated geometrical changes upon ionization, one expects the strong fundamentals of the C(1)−C(2) and C(1)−Br stretching vibrations, modes 5 and 12, respectively. Indeed, they appear prominently at 1493 and 787 cm^{-1} in the MATI spectrum, respectively, close to 1484 and 765 cm^{-1} predicted at the BP86 level. There appear other prominent a'-type fundamentals also, namely, those of modes 6, 8, 13, and 14 at 1402, 1267, 370, and 238 cm^{-1}, respectively, which can be readily assigned by comparison with the DFT frequencies. Their prominence cannot be predicted simply on the basis of the geometrical changes upon ionization. However, the calculated Franck−Condon factors listed in Table 5 are large for all of these transitions, aiding their positive identification. Of the eight remaining a' fundamentals, those of the CH stretching modes (1∼4) are expected to be very weak, even though the very weak peak at 2970 cm^{-1} might be assigned to the ν_4 fundamental. The theoretical Franck−Condon factors also predict very weak intensities for the fundamentals of modes 7, 9, 10, and 11, which can be assigned to the very weak peaks at 1308, 1194, 1124, and 942 cm^{-1}, respectively.

The prominence of the fundamentals of modes 5, 6, 8, 12, 13, and 14 suggests noticeable overtones of these modes. The first overtones of all of these modes could be identified as listed in Table 5. In addition, the combinations involving these modes are expected to be distinct, especially those involving modes 12, 13, and 14, as predicted by the calculated Franck−Condon factors. Hence, 12^113^1, 12^114^1, and 13^114^1 can be assigned to the distinct peaks at 1157, 1026, and 608 cm^{-1}, respectively, on the basis of the calculated frequencies and Franck−Condon factors. Many other combinations involving these can be easily assigned also, such as 6^114^1 and 5^114^1 involving mode 14; 8^113^1, 6^113^1, and 5^113^1 involving mode 13; and 8^112^1, 6^112^1, and 5^112^1 involving mode 12. In fact, most of the weak peaks in the MATI spectrum could be assigned to the combinations involving modes 5, 6, 8, 12, 13, and 14 as listed in Table 5.

Even though the first overtones of the a''-type modes are electric dipole-allowed, the calculated Franck−Condon factors were very small (10^{-4} or less) for those of modes 15∼19. The a' combinations involving these had very small Franck−Condon factors also. None of these could be identified in the MATI spectrum, in agreement with the theoretical prediction. The fundamentals of some of these appeared, even though very weakly, in the MATI spectrum, probably via vibronic mechanism. For example, the very weak shoulder peak at 752 cm^{-1} was assigned to the ν_{19} fundamental because BP86 and B3LYP predict 745 and 780 cm^{-1} for this mode. If the reliability of the DFT results as demonstrated for the a' peaks is accepted, no alternative assignment would be more reasonable than the above.

Left unassigned are the weak low-frequency peaks at 141, 154, 276, and 303 cm^{-1}, which can be the fundamentals of modes 20 (out-of-plane bending) and 21 (CH_3 torsion). Even though the calculated harmonic frequency of the mode 21 fundamental is higher than that of mode 20, its quantum mechanical frequency (anharmonic) is comparable to the latter. We tentatively assign the peaks at 141 and 276 cm^{-1} to 20^1 and 20^2 and those at 154 and 303 cm^{-1} to 21^1 and 21^2, respectively, even though the other way around is equally plausible. The assignments for the combinations involving modes 20 and 21 in Table 5 are also tentative.

2. *cis*-1-C_3H_5Br. The overall spectral features of the *cis*-1-C_3H_5Br cation are rather similar to those of the trans isomer. The fundamentals of the CH stretching modes, 1∼4, are hardly observable. Among the remaining a'-type fundamentals, modes 5, 6, 7, 12, and 13 appear prominently at 1506, 1397, 1263, 743, and 519 cm^{-1}, respectively, in agreement with the calculated frequencies. Calculated Franck−Condon factors are large for these fundamentals also. Unlike trans, 14^1 appears weakly at 204 cm^{-1} in the cis spectrum, while 9^1 is stronger than in trans. Then, most of the minor peaks in the MATI spectrum would be the overtones or the combinations of modes 5, 6, 7, 9, 12, and 13. The participation of mode 13 in these, and mode 12 to a lesser extent, is expected to be rather extensive on the basis of the intensity of the fundamentals. Accordingly, distinct overtones 13^2 and 13^3 are observed at 1039 and 1556 cm^{-1}, respectively, and 12^2 and 12^3 at 1484 and 2219 cm^{-1} with lesser intensities. It is to be emphasized that the above assignments are highly likely in the sense that no alternative assignments can be made when references are made to the DFT frequencies listed in Table 6. The distinct combinations involving mode 13 are 12^113^1, 9^113^1, 7^113^1, 6^113^1, and 5^113^1 at 1263, 1751, 1776, 1913, and 2030 cm^{-1}, respectively. Those involving mode 12 are less distinct, 9^112^1, 7^112^1, 6^112^1, and 5^112^1 at 1985, 1985, 2137, and 2255 cm^{-1}, respectively. The peak at 1985 cm^{-1} may be the overlapping band of 9^112^1 and 7^112^1 on the basis of the calculated frequencies and the Franck−Condon factors.

Some a''-type fundamentals are also observed, even though weakly. These are 16^1, 17^1, 18^1, 19^1, and 20^1 at 1341, 984, 804, 706, and 235 cm^{-1}, respectively. All of these lie between the two DFT frequencies. The torsional fundamental for the cis cation is expected to have the lowest frequency among the normal modes. This cannot be positively identified in the MATI spectrum because there is hardly any signal in the 100∼150 cm^{-1} region where it is expected. An extremely small Franck−Condon factor must be responsible for its absence. The first overtone of this mode is electric dipole-allowed, however. In fact, 21^2 is the only plausible assignment for the peak at 223 cm^{-1}. Since its frequency is significantly smaller than the calculated value, the frequency of 21^1 is also expected to be less than the calculated frequency of ∼140 cm^{-1}. Assigning the very weak peak at 347 cm^{-1} to 20^121^1, the frequency of 21^1 becomes ∼112 cm^{-1}, in agreement with the above argument. It is to be mentioned that there is no reasonable alternative assignment for the peak at 347 cm^{-1}.

A final question to be answered is that 14^1 is weak in the cis spectrum while the same peak is the second strongest for trans. The simple qualitative argument based on the geometrical changes upon ionization cannot explain the dramatic difference in the two cases. Since the calculated Franck−Condon factors correctly predict the above difference, an answer must be found from the molecular properties affecting the magnitude of this factor. We looked into the matrixes and the vectors obtained in the calculation of the Franck−Condon factors. It was found that the **J** matrixes in eq 1 were similar for the trans and cis isomers while the **K** vectors were significantly different. In particular, the 14th component of the latter for trans, which is the effective

geometrical change along the mode 14 eigenvector, was larger by around three than that of cis, which resulted in almost an order of magnitude difference in 14^1 intensities. Getting into the details, the main contributors to the mode 14 eigenvector of trans were the internal eigenvectors along the ∠BrC(1)C(2) and ∠C(1)C(2)C(3) bond angles and the geometrical change along ∠BrC(1)C(2) made main contribution to the 14th component of **K**. In addition to the changes along these bond angles, the geometrical change along the C(1)C(2) bond length was also important for cis, which more or less canceled the contribution from ∠BrC(1)C(2) and resulted in smaller 14th component. To summarize, eigenvectors did not change much upon ionization for both isomers. However, the eigenvectors of mode 14 were a little different for the two isomers, which eventually led to the dramatically different intensities of 14^1 in the two cases.

V. Summary and Conclusion

Compared to the usual two-photon scheme for ZEKE/MATI, the main advantage of the one-photon scheme is the capability to detect strong signals even when an appropriate excited electronic state is not easily accessible. The MATI spectroscopic studies of *trans*- and *cis*-1-C_3H_5Br presented in this paper are cases in point. It may be thought that the unavailability of the information on the final state accessible through the intermediate-state selection in the two-photon scheme would be a handicap of the one-photon scheme. We have demonstrated in this work, and in previous ones, that such a difficulty can be largely overcome by utilizing the frequencies and the Franck−Condon factors obtained by quantum chemical calculations. In particular, the DFT results have been found to provide a powerful guideline for spectral assignment. For example, the DFT results correctly predicted the widely different intensities of 14^1 of the trans and the cis isomers, which are totally unexpected.

In our previous MATI investigation of 2-C_3H_5Br, a rich spectral feature was found close to the 0-0 band, which could be assigned to irregular torsional overtones through quantum mechanical calculations. The torsional vibration behaved rather regularly in the present cases because the related barriers were much higher than that of the 2-C_3H_5Br cation. Namely, the fundamentals were either very weak or absent while the overtones were more distinct. Regardless, the torsional energy levels calculated quantum mechanically were different from those estimated from the harmonic frequencies even when the barriers were as high as several hundred cm^{-1}. In this regard, care must be taken in the assignments of torsional peaks.

Acknowledgment. This work was financially supported by CRI, the Ministry of Science and Technology, Republic of Korea. M.L. thanks the Ministry of Education for the Brain Korea 21 fellowship.

References and Notes

(1) Müller-Dethlefs, K.; Sander, M.; Schlag, E. W. *Chem. Phys. Lett.* **1984**, *112*, 291.
(2) Fischer, I.; Lindner, R.; Müller-Dethlefs, K. *J. Chem. Soc., Faraday Trans.* **1994**, *90*, 2425.
(3) Merkt, F.; Softley, T. P. *J. Chem. Phys.* **1995**, *103*, 4509.
(4) Hepburn, J. W. *Chem. Soc. Rev.* **1996**, *25*, 281.
(5) Kimura, K. *J. Elec. Spectrosc. Relat. Phenom.* **2000**, *108*, 31.
(6) Zhu, L.; Johnson, P. *J. Chem. Phys.* **1991**, *94*, 5769.
(7) Krause, H.; Neusser, H. J. *J. Chem. Phys.* **1992**, *97*, 5923.
(8) Lin, J. L.; Lin, K. C.; Tzeng, W. B. *J. Phys. Chem. A* **2002**, *106*, 6462.
(9) Park, S. T.; Kim, S. K.; Kim, M. S. *J. Chem. Phys.* **2001**, *114*, 5568.
(10) Kwon, C. H.; Kim, H. L.; Kim, M. S. *J. Chem. Phys.* **2003**, *118*, 6327.
(11) Kwon, C. H.; Kim, H. L.; Kim, M. S. *J. Chem. Phys.* **2003**, *119*, 215.
(12) Park, S. T.; Kim, S. K.; Kim, M. S. *Nature* **2002**, *415*, 306.
(13) Park, S. T.; Kim, M. S. *J. Am. Chem. Soc.* **2002**, *124*, 7614.
(14) Herzberg, G. *Molecular Spectra and Molecular Structure III*; Van Nostrand: Princeton, NJ, 1966.
(15) Jacox, M. E. *J. Phys. Chem. Ref. Data* **1998**, *27* (2), 115.
(16) Lee, M.; Kim, M. S. *J. Chem. Phys.* **2003**, *119*, 5085.
(17) Lee, M.; Kim, M. S. *J. Chem. Phys.* **2003** (in press).
(18) Ng, C. Y. *Annu. Rev. Phys. Chem.* **2002**, *53*, 101.
(19) Seiler, R.; Hollenstein, U.; Softley, T. P.; Merkt, F. *J. Chem. Phys.* **2003**, *118*, 10024.
(20) Woo, H. K.; Zhan, J.; Lau, C. K.; Ng, C. Y.; Cheung, Y. S. *J. Chem. Phys.* **2002**, *116*, 8803.
(21) Moss, D. B.; Parmenter, C. S. *J. Chem. Phys.* **1993**, *98*, 6897.
(22) Timbers, P. J.; Parmenter, C. S.; Moss, D. B. *J. Chem. Phys.* **1994**, *100*, 1028.
(23) Lin, C. C.; Swalen, J. D. *Rev. Mod. Phys.* **1959**, *31*, 841.
(24) Spangler, L. H. *Annu. Rev. Phys. Chem.* **1997**, *48*, 481.
(25) Lu, K. T.; Weinhold, F.; Weisshaar, J. C. *J. Chem. Phys.* **1995**, *102*, 6787.
(26) Takazawa, K.; Fujii, M.; Ito, M. *J. Chem. Phys.* **1993**, *99*, 3205.
(27) Samson, J. A. R. *Techniques of Vacuum Ultraviolet Spectroscopy*; Wiley: New York, 1967.
(28) Frisch, M. J.; Trucks, G. W.; Schlegel, H. B.; Scuseria, G. E.; Robb, M. A.; Cheeseman, J. R.; Zakrzewski, V. G.; Montgomery, J. A., Jr.; Stratmann, R. E.; Burant, J. C.; Dapprich, S.; Millam, J. M.; Daniels, A. D.; Kudin, K. N.; Strain, M. C.; Farkas, O.; Tomasi, J.; Barone, V.; Cossi, M.; Cammi, R.; Mennucci, B.; Pomelli, C.; Adamo, C.; Clifford, S.; Ochterski, J.; Petersson, G. A.; Ayala, P. Y.; Cui, Q.; Morokuma, K.; Malick, D. K.; Rabuck, A. D.; Raghavachari, K.; Foresman, J. B.; Cioslowski, J.; Ortiz, J. V.; Stefanov, B. B.; Liu, G.; Liashenko, A.; Piskorz, P.; Komaromi, I.; Gomperts, R.; Martin, R. L.; Fox, D. J.; Keith, T.; Al-Laham, M. A.; Peng, C. Y.; Nanayakkara, A.; Gonzalez, C.; Challacombe, M.; Gill, P. M. W.; Johnson, B.; Chen, W.; Wong, M. W.; Andres, J. L.; Gonzalez, C.; Head-Gordon, M.; Replogle, E. S.; Pople, J. A. *Gaussian 98*, revision A.6; Gaussian Inc.: Pittsburgh, PA, 1998.
(29) Sharp, T. E.; Rosenstock, H. M. *J. Chem. Phys.* **1964**, *41*, 3453.
(30) Chau, F.; Dyke, J. M.; Lee, E. P.; Wang, D. *J. Elec. Spectrosc. Relat. Phenom.* **1998**, *97*, 33.
(31) Lewis, J. D.; Malloy, T. B., Jr.; Chao, T. H.; Laane, J. *J. Mol. Struct.* **1972**, *12*, 427.
(32) Bauder, A.; Mathier, E.; Meyer, R.; Ribeaud, M.; Günthard, H. H. *Mol. Phys.* **1968**, *15*, 597.
(33) Beaudet, R. A. *J. Chem. Phys.* **1969**, *50*, 2002.
(34) Elst, R.; Berg, G. C. v. d.; Oskam, A. *Recueil* **1972**, *91*, 417.
(35) Neugebauer, J.; Hess, B. A. *J. Chem. Phys.* **2003**, *118*, 7215.
(36) Watanabe, K.; Nakayama, T.; Mottl, J. *J. Quant. Spectrosc. Radiative Transfer* **1962**, *2*, 369.
(37) Reiser, G.; Rieger, D.; Wright, T. G.; Müller-Dethlefs, K.; Schlag, E. W. *J. Phys. Chem.* **1993**, *97*, 4335.
(38) Wright, T. G.; Panov, S. I.; Miller, T. A. *J. Chem. Phys.* **1995**, *102*, 4793.
(39) Worrell, C. W. *J. Elec. Spectrosc. Relat. Phenom.* **1974**, *3*, 359.
(40) Kimura, K.; Katsumata, S.; Achiba, Y.; Yamazaki, T.; Iwata, S. *Handbook of HeI Photoelectron Spectra of Fundamental Organic Molecules*; Japan Scientific Societies Press: Tokyo, 1981.